Noble metal promoted CoMn catalysts for Fischer-Tropsch synthesis

Eirik Østbye Pedersen[1] and Edd A. Blekkan*[1]

[1]Department of Chemical Engineering, Norwegian University of Science and Technology, 7491 Trondheim, Norway
*Corresponding author: edd.a.blekkan@ntnu.no

January 9, 2018

Abstract

Noble metal (Pt, Re and Ru) promoters were investigated for Fischer-Tropsch synthesis at light olefin favouring conditions over Co–Mn catalysts. Characterisation and testing found promotion to increase catalyst activity without compromising the selectivity promoting effects of Mn. The noble metal promoted catalysts showed olefin and C_{5+} selectivities that were slightly increased compared to the unpromoted catalysts indicating some degree of influence on the selectivity.

Keywords:

- Fischer-Tropsch, Cobalt, Manganese, Platinum, Rhenium, Ruthenium.

Highlights:

- Mn promotion increases selectivity towards C_{2-4} olefins and C_{5+} and also decreases selectivity towards CH_4.
- Mn promotion has negative effect on reducibility, limiting the activity of the catalyst.
- Additional noble metal promotion reverses the negative effect of Mn on reducibility, increasing activity without compromising selectivity.

1. Introduction

Fischer-Tropsch synthesis (FTS) remains a staple of the gas-to-liquids (GTL) processes that utilise carbon in the form of coal, biomass or natural gas to produce fuels and chemicals. In the FTS process, synthesis gas (CO and H_2) are converted into hydrocarbons over a solid catalyst via a surface polymerisation reaction. The hydrocarbon products are primarily *n*-paraffins and α-olefins of various lengths and to lesser degrees branched isomers and oxygenates [1, 2].

The produced hydrocarbons are typically used as high-quality transportation fuels after upgrading, and due to their chemical composition, they are particularly well suited as feedstock for diesel and aviation fuel production. More recent market developments have also lead to FTS being proposed as a potential alternative for light olefin production with high selectivities for olefins being reported [3–5] using specialised catalysts and operating conditions.

The Fischer-Tropsch can be performed by Fe, Co, Ni and Ru catalysts, but due to the scarcity and price of Ru and the high methanation activity of Ni, Fe and Co are the most commonly employed. Co is generally chosen for its high activity and selectivity to long chain hydrocarbons and is preferred when using syngas with a high H_2/CO ratio as that originating from natural gas [6]. To enhance the properties of FTS catalysts, they are typically promoted. Promoter elements can roughly be divided into two categories. *Structural promoters* affect the formation and stability of the catalyst active phase, while *electronic promoters* directly affect the intrinsic properties of the catalyst by influencing the local electronic structure of the active metal [7].

Manganese as a promoter has a range of reported properties and can be regarded as both a structural and electronic promoter. Its properties seem to depend strongly on how the catalyst was prepared and which support material was used [4, 8, 9]. In many cases, an increased selectivity to C_{5+} species, increased olefin/paraffin ratio and a decreased selectivity to CH_4 is reported [8, 10–13] along with an increased intrinsic activity [8, 9, 14, 15]. Because of these properties, Mn is frequently employed as a promoter for obtaining light olefins. Moreover, Mn is often reported to negatively affect Co reducibility which may

have an adverse effect on the available metallic Co area [8, 13, 15, 16].

Noble metal promoters are generally considered structural promoters, their main property to decrease the reduction temperature of Co and increase the metallic Co surface area. Among them, Pt, Re and Ru are the most studied [7].

Re is generally regarded as a wholly structural promoter. It has been reported to increase the reducibility of Co via a H_2 spillover effect and increase the available $Co^{(0)}$ surface area. It is not assumed to increase intrinsic activity, but has been reported to increase C_{5+} selectivity [7, 17].

Pt is also a structural promoter, reported to increase metallic surface area of Co catalysts and not affect intrinsic activity [17, 18]. Some adverse effects on CH_4 and C_{5+} selectivity have however been reported [17, 19].

Ru is the most studied of all noble metal FTS promoters. Being a highly active FTS catalyst in its own right it has been reported to possess both structural and electronic promotional properties [7]. Increasing the metallic Co surface area similarly to Pt and Re, Ru has also been shown to have synergistic effects with Co [20], significantly increasing activity and C_{5+} selectivity.

In the present work, Mn-promoted Co catalysts will be investigated for the purpose of Fischer-Tropsch synthesis. Mn-promotion will be combined with promotion with Pt, Re or Ru to see if the noble metals will be able to counter the negative effects of Mn addition without compromising the positive ones. Catalysts will be synthesised, characterised and tested for the FTS at industrially relevant conditions favouring light olefin formation.

2. Methods

2.1 Catalyst Synthesis

All catalysts investigated were prepared by the incipient wetness impregnation (IWI) method using $Co(NO_3)_2 \cdot 6H_2O$ and $Mn(NO_3)_2 \cdot 4H_2O$, as well as $Pt(NH_3)_4(NO_3)_2$, $HReO_4$(aq.) and $Ru(NO)(NO_3)_3$ in dilute nitric acid precursors

and γ-Al_2O_3 (S_{BET} = 175 m^2/g) as the support material.

Following the optimised results from our previous work [8], the catalysts were prepared in two steps: First Mn was impregnated, then the catalyst was dried overnight under reduced pressure and calcined in flowing air at 300 °C (2 °C/min) for 16 h. Then Co together with the respective noble metal (NM) was impregnated and the drying and calcination processes were repeated. Additionally, a CoMn catalyst without NM as well as a Co catalyst without Mn or NM were prepared to serve as references. For all catalysts the nominal Co, Mn and NM loadings were kept constant at 15, 3.75 and 0.5 %wt. respectively. It was assumed that Mn was exclusively present as MnO_2 after the first preparation step [9]. Prior to further characterisation and testing, all catalysts were sieved to a particle size range of 53-90 µm.

2.2 Catalyst Characterisation

All catalysts were characterised by temperature programmed reduction on an Altamira Instruments^{TM} AMI-300RHP instrument with a temperature profile of 10 °C/min to 900 °C in 7% H_2/Ar flow. Degrees of reduction (DoR) were also estimated by performing TPR on *in situ* pre-reduced catalysts and comparing integrated profiles for calcined and pre-reduced samples. To determine catalyst dispersion, volumetric H_2-chemisorption experiments were carried out on a Micromeritics ASAP 2020 C at 40 °C on *in situ* reduced samples.

X-ray diffraction (XRD) experiments were performed at ambient temperature on a Bruker D8 Advance DaVinci diffractometer using a CuKα X-ray tube. Lattice parameters and average particle sizes were determined for Co_3O_4 using the Pawley [21] method of full pattern refinement in the Bruker.Diffrac Topas 5.0 software [22]. A separate scan of pure γ-Al_2O_3 was fitted and incorporated in the refinement. Co$^{(0)}$ particle sizes were estimated by multiplying Co_3O_4 particle size by 0.75, and dispersion was estimated using the formula D = 96/d, were D is Co dispersion (%) and d in average particle size (nm) [23].

A more detailed description of the characterisation methods can be found in our previous work [8].

2.3 Quantitative elemental analysis

Quantitative analysis of Al, Co, Mn, Pt, Re and Ru was carried out by Inductively Coupled Plasma Mass Spectrometry (ICP-MS). Prior to analysis, the samples (20

4

mg) was digested by ultrasonic agitation for 2 h at 80 °C in 3 mL aqua regia, then diluted to 220 mL with ultra-pure water. The resulting solution was analysed by a ThermoScientific ELEMENT 2$^{\text{TM}}$ ICP-MS instrument.

2.4 Fischer-Tropsch Synthesis

Fischer-Tropsch Synthesis was performed in a 10 mm I.D. tubular stainless steel fixed bed reactor at 240 °C, 5 bara and $H_2/CO = 2.1$. The catalyst (1 g) was diluted with inert SiC (19 g) to minimise temperature gradients and loaded into the reactor between plugs of quartz wool to keep the catalyst bed in place. The reactor was fixed in an aluminium block to further facilitate heat distribution and mounted in a furnace. The catalysts were then reduced *in situ* in 125/125 mL/min H_2/He at 350 °C (1 °C/min) for 16 h. The reactor was then pressurised in He flow to 5 bar at 180 °C before syngas (250 mL/min) was introduced. Subsequently, the reactor was heated to 230 °C (20 °C/h) and 240 °C (5 °C/h). Effluent gases were passed through a hot trap kept at approx. 100 °C and a cold trap at ambient temperature before the gas phase was analysed by an Agilent Technologies 6890N GC fitted with a TCD and an FID. The syngas contained 3 %vol. N_2 which served as the GC internal standard. Catalyst activity was compared at equal syngas space velocity at approx. 16 h time on stream. After 24 h, the space velocity was adjusted to compare selectivity at equal CO conversion levels of 50 ± 2 %.

3. Results and discussion

3.1 ICP-MS

The results from the elemental analysis are shown in Table 1. It can be seen that the estimated Al concentrations are lower than the nominal values of 39-43 %wt. This is probably due to incomplete digestion of the sample where a portion of the Al_2O_3 is left undissolved. This is reflected in the measured Co:Al ratios which are significantly higher than the nominal values of 0.33-0.35. As apparently not all the catalyst mass is dissolved, observing relative concentrations rather than absolute concentrations seems more practical. The measured Mn:Co ratios are near identical to the nominal value (0.25). The Pt and Re concentrations are also close (0.033), but a near 50 % loss of Ru is observed. Ru has been known to

5

form volatile oxides during oxidative treatments [24] and is likely lost during calcination. This effect seems enhanced by the presence of nitrates [25,26], so that is probably why our observed loss is so substantial, as nitrates are provided in the form of both $Co(NO_3)_2$, $Ru(NO)(NO_3)_3$ and HNO_3.

3.2 TPR

TPR profiles are presented in Fig. 1 with peak temperatures and calculated DoRs listed in Table 2. Three peaks are observed in the experiments. The first, evident as a shoulder at around 150 - 250 °C for all catalysts except CoMnRu, is generally attributed to the reduction of residual nitrates from calcination [23] while the two latter, at 250 - 330 °C and 400 - 500 °C respectively, originate from the stepwise reduction of Co_3O_4 [27]. Additionally, a small peak is observed for the CoMn catalyst at approx. 390 °C. In our previous work [8], we found the reduction of supported Mn to have a small peak at around this temperature, so this may be caused by the reduction of MnO_2 separated from Co. Besides this feature, the CoMn profile is very similar to that of the Co reference. Comparing the profiles of the pre-reduced Co and CoMn catalysts, they are equally positioned, but the CoMn profile is slightly larger resulting in a lower DoR.

All NM promoted catalysts display significant improvement is reducibility. Peak positions are generally shifted towards lower temperatures, and the peaks for the pre-reduced catalysts are lower in intensity. Consequently, a significant increase from 70 to over 90 % in the estimated DoR is observed for all NM promoted catalysts. For the Pt and Ru promoted catalysts, both main reduction peaks are shifted towards lower temperatures, but for the Re promoted catalyst, only the $CoO{\rightarrow}Co^{(0)}$ peak is shifted. This is in accordance with existing literature and has been attributed to Re existing in oxidic form until after the reduction of $Co_3O_4{\rightarrow}CoO$, and the reducibility enhancing effects of Re being exclusive to $Re^{(0)}$ [18,28]. Despite its near 50 % loss, Ru appears to be the strongest reduction promoter with the smallest peak and the lowest reduction temperature for the pre-reduced run resulting in the highest estimated DoR of 97 %.

3.3 Dispersion

Measured dispersions and particle sizes are shown in Table 2. For the H_2-chemisorption measured dispersions, significant differences are observed

6

between the catalysts with results ranging from 4.8 to 7.5 %. The CoMn catalyst displays a lower dispersion than the unpromoted catalyst, while the NM promoted catalysts exhibits the highest dispersions. In comparison, the estimated particle sizes and dispersions based on XRD vary to a much lesser extent, indicating that the differences in H_2 uptake/$Co^{(0)}$-surface area are not caused by differing Co particle sizes. Our previous results [8] indicated that Mn required good contact with Co to exhibit promotion effects, but Mn incorporation in the Co_3O_4 lattice limits catalyst reducibility and, as a consequence, the available $Co^{(0)}$ surface area. With Mn promotion we observe a slight increase in the Co_3O_4 lattice parameter (Table 2) indicating at least some degree of Mn incorporation in the Co_3O_4 lattice. In the XRD patterns shown in Fig 2 there is also a weak, but observable signal from MnO_2 at $2\theta = 28.7$, 44.8 and 55.7°, indicating separate Co and Mn phases. Further promotion with NM does not seem to have any noticeable effect on the degree of Mn incorporation in the Co_3O_4 lattice.

In our previous work [8], we observed a good correlation between the estimated DoRs and dispersions based on H_2-chemisorption. A similar correlation is observed here as well, indicating that the effect of Mn on Co dispersion is by limiting the reducibility of Co and thus the available $Co^{(0)}$surface area.

The presented dispersions based on H_2 chemisorption are based on the assumption that only Co adsorbs any H_2. While Mn in its likely oxidic form does not adsorb hydrogen [8], all the investigated NMs are known hydrogenation catalysts capable of adsorbing hydrogen which may cause an overestimation of the dispersion.
fits (red) normalised to the γ-Al_2O_3 peak at $2\theta = 66.9°$.

3.4 Fischer-Tropsch Synthesis

The Co-specific activity and intrinsic activity for the catalysts in the initial 24 h of operation are presented in Fig. 3. The catalyst performance varies from 0.4 - 0.7 $mol_{CO}/g_{Co}\cdot h$, with the CoMn catalyst displaying the lowest activity and CoMnRe and CoMnRu the highest. The CoMn catalyst displays the poorer Co-specific activity compared to the unpromoted catalyst, and all the NM promoted catalysts have higher activities. Comparing the site-time yields, results vary in a rather narrow range, approx. 0.14 - 0.18 s^{-1}. Except for the Re-promoted catalyst, which displays a higher activity than the rest, all catalysts are close in performance, with the unpromoted catalyst displaying the poorest activity.

In our previous work [8], Mn promotion was found to enhance the intrinsic

activity by approx. 50 % and also display a higher Co specific activity compared to the Co reference. No such effect is seen here, and considering the TPR results it is possible that the Co-Mn contact obtained in this work is not as good as before, possibly due to a different support used with stronger Mn interaction. Re promotion appears to undo this to a certain degree with the Re catalyst displaying a significantly higher intrinsic activity than the rest. Re is generally not believed to enhance the intrinsic activity of Co catalysts [17], so two possible explanations exist for this observation. It is suggested that decoration of the Co surface is responsible for activity enhancing effect of Mn [14]. So it is possible that CoMnRe is the only catalyst with notable Mn decoration of the Co surface which improves its intrinsic activity. Partial Mn blockage of the Co surface would also explain why it has the same dispersion as CoMnPt despite having smaller Co_3O_4 particles, as analysed by XRD.

There might also be a weakness in the estimation of the catalysts' dispersions. Observing the Co-specific activity, the activity enhancing properties of the NM promoters are more comparable, with CoMnPt's activity slightly lower due to its larger particle size. However, based on the H_2-chemisorption, CoMnPt has the same dispersion as CoMnRe despite having the same DoR and larger particle size. Re promotion in Co catalysts has been studied previously with *in situ* XAS, and Re has been found to be atomically dispersed in the Co [29] particles under operating conditions. As such, it is unlikely to contribute to hydrogen uptake. Similar results have however also been observed for Pt [30, 31], but XPS studies have suggested Pt to become enriched at the metallic Co surface after reduction [32, 33]. As such, it would possibly have an effect on the adsorptive properties of H_2. Ru as well has been found to be enriched at the metallic cobalt surface after reduction, modifying the adsorption properties of the $Co^{(0)}$ sites [34]. Pt and Ru could affect the adsorption properties of H_2 in a different manner from Re, and consequently, an overestimation of the Pt and Ru promoted catalyst's dispersion is a possible cause of the observed differences in intrinsic activity.

The selectivity results are presented in Fig. 4 and gas-phase α-olefin/*n*-paraffin ratios are shown in Fig. 5. For all Mn-promoted catalysts, a marked drop in selectivity to CH_4 of 5 - 6 % is observed when compared to Co. This is coupled with an increase in C_{5+} selectivity of approx. 6 %. The C_{2-4} fraction is slightly smaller, but considerably more olefinic as evidenced by the up to 2.5-fold increase in O/P ratio shown in Fig. 5. The selectivity to C_4 iso-olefins is also slightly reduced with Mn promotion, and the selectivity to CO_2 remains low,

8

under 1 %, for all catalysts.

The Mn affected selectivities are in line with what has been observed previously. The lowered selectivity to CH_4 and heightened selectivity to C_{5+} species are consistent with what is generally reported with Mn promotion. The increased selectivity towards olefinic products is also in line with most available literature [8, 10–13]. Interestingly, the Mn enhanced selectivity is about the same here as in our previous work [8] whereas the activity is not. This could mean that the selectivity effect requires a different type of Co-Mn contact than the activity. Mn decoration of the Co surface has previously been a proposed promotion effect, and the Co-Mn interface sites being the source of the enhanced activity [14]. If this is the case, it would seem that the enhanced selectivity is the result of a longer range electronic effect.

Two possible explanations exist for the effect of Mn on olefin selectivity. The first is to decrease the adsorption energy of olefins. Olefin adsorption energy has been identified as a key descriptor for determining olefin selectivity [35, 36]. A lowering of the adsorption energy of olefins would in turn increase the probability of olefin desorption relative to hydrogenation or chain growth. It would also decrease the probability of olefin re-adsorption which leads to hydrogenation, chain growth and isomerisation [37]. As the iso-olefin selectivity is lowered with Mn promotion here, this lends some credibility to Mn lowering adsorption energy of olefins. However, DFT calculations have shown that Mn addition increases the binding energy of most species [8, 38–40]. It should be noted that these calculations have however been performed on metallic Mn rather than MnO, which is the likely operating state of Mn [11].

The second explanation is an inhibited hydrogenation activity, either by displacement of H_2, or by unfavourable affecting the energetics of elementary hydrogenation reactions. In our previous work [8], using DFT, we found the latter to be true for the hydrogenation of CH_2 and CH_3. There is a possibility that the same applies for olefins and higher alkyls as well. A previous SSITKA investigation found Mn to increase the surface coverage of CH_x [41]. This was correlated with increased C_{5+} and lowered CH_4 selectivity without mention of olefins. From our results [8] and others [42,43], increased C_{5+} and lowered CH_4 selectivity has been found to correlate with increased olefin selectivity and been attributed to olefin reinsertion, so an increased surface coverage of CH_x, (i.e. displacement of H_2), is a likely explanation for the increased olefin selectivity as

well.

As with the activity results, the promotion effect appears to be further enhanced (however slightly), by NM promotion. The effect of Ru is slightly lower than for Pt and Re, likely due to the fact that its loading is about half that of Pt and Re. Although NM promoters are mostly used for their activity enhancing effects, they are also known to have a range of effects on catalyst selectivity. Previous studies have reported that Pt has no effect on selectivity [18, 44], as well as shifting the selectivity to lighter products [17, 19]. Re has been found to slightly increase the C_{5+} and decrease CH_4 selectivity [17], while Ru has also been found to have no effect [34] on selectivity, as well as positive effects on C_{5+} selectivity [20]. Detrimental effects seem most apparent at high ($\geq$ 1 %) NM loadings [19], which may explain why none are seen in this work. Positive effects require intimate NM-Co contact [20] to achieve synergistic effects.

A prerequisite for observable Mn promotion effects in Co catalysts is good Co-Mn contact [8, 9]. Rather than directly influencing the Co, the NM promotion may facilitate this in some manner. This may be a result of the enhanced reduction of Co, or some direct Co-Mn-NM interaction. Mn-support interaction has previously been pointed out as a key factor in limiting Co-Mn contact [8, 13]. Pt has previously been shown to hinder the formation of $CoAl_2O_4$ [30]. If Pt also hinders support interaction with Mn, this would in turn facilitate Co-Mn contact. A similar effect from the other NMs may be a possible explanation for the observed selectivity effects.

In our case, the selectivity differences between the CoMn catalyst and the NM promoted CoMn catalysts are likely too small to make a conclusive remark. The most significant measured difference between them is the enhanced DoR which would indicate that the most likely explanation for the observed selectivity effects is enhanced Co-Mn contact due to the increased reduction of Co. However, the weakest NM promotion effect is seen with Ru which gave the highest DoR despite having 50 % of the loading as Pt and Re indicating at least some degree of direct NM influence on the Co selectivity.

4. Conclusion

Noble metal (NM) promotion in the form of Pt, Re and Ru, was investigated in CoMn catalysts for Fischer-Tropsch synthesis at light olefins favouring

conditions, and compared to both a CoMn and Co catalyst without NM promotion. For all NM promoted catalysts, an increase in the degree of reduction was observed as well as an increase in dispersion determined by H_2-chemisorption. The Co-specific reaction rate increased in the order CoMn < Co < CoMnPt < CoMnRe c CoMnRu, while in terms of intrinsic activity, CoMnRe was the most active and the rest were similar in performance. This was ascribed to poor Co-Mn contact in the CoMn catalyst, which was improved upon NM addition. The intrinsic activity of CoMnPt and CoMnRu was likely underestimated due to Co-NM interaction during the dispersion estimation. Compared to Co, the CoMn catalyst displayed heightened selectivity to C_{2-4} olefins and C_{5+} species as well as lowered selectivity to CH_4. These effects were slightly enhanced with the addition of NM, but the source of the NM enhancement effect was unclear.

Acknowledgements

References

[1]   M.E. Dry, in: Handbook of Heterogeneous Catalysis, eds. G. Ertl, H. Knözinger F. Schüth and Jens Weitkamp (Wiley-VCH, 2008) ch. 13.15.

[2]   T. Kaneko, F. Derbyshire, E. Makino, D. Gray, M. Tamura, K. Li,

Coal Liquefaction in Ullmann's Encyclopedia of Industrial Chemistry (Wiley-VCH, 2012).

[3] Torres Galvis HM, Bitter JH, Khare CB, Ruitenbeek M, Dugulan AI, de Jong KP (2012) Science 335:835.

[4] Torres Galvis HM de Jong KP (2013) ACS Catal 3:2130.

[5] Zhong L, Yu F, An Y, Zhao Y, Sun Y, Li Z, Lin T, Lin Y, Qi X, Dai Y, Gu L, Hu J, Jin S, Shen Q, Wang H (2016) Nature 538:84.

[6] Khodakov AY, Chu W, Fongarland P (2007) Chem Rev 107:1692.

[7] Morales F, Weckhuysen BM (2006) Catalysis 19:1.

[8] Østbye Pedersen E, Svenum IH, Blekkan EA (2017) Submitted.

[9] Morales F, Grandjean D, Mens A, de Groot FMF, Weckhuysen BM (2006) J Phys Chem B 110:8626.

[10] Cano FM, Gijzeman OLJ, de Groot FMF, Weckhuysen BM (2004) Stud Surf Sci Catal 147:271.

[11] Morales F, de Groot FMF, Glatzel P, Kleimenov E, Bluhm H, Hävecker M, Knop-Gericke A, Weckhuysen BM (2004) J Phys Chem B 108:16201.

[12] Morales F, de Smit E, de Groot FMF, Visser T, Weckhuysen BM (2007) J Catal 246:91.

[13] Bezemer GL, Radstake PB, Falke U, Oosterbeek H, Kuipers HPCE, van Dillen AJ, de Jong KP (2006) J Catal 237:152.

[14] Johnson GR, Werner S, Bell AT (2015) ACS Catal 5:5888.

[15] Shimura K, Miyazawa T, Hanaoka T, Hirata S (2015) Appl Catal, A 494:1.

[16] Morales F, de Groot FMF, Gijzeman OLJ, Mens A, Stephan O, Weckhuysen BM (2005) J Catal 230:301.

[17] Ma W, Jacobs G, Keogh RA, Bukur DB, Davis BH (2012) Appl Catal, A 437-438:1.

[18] Vada S, Hoff A, Ådnanes E, Schanke D, Holmen A (1995) Top Catal 2:155.

[19] Jermwongratanachai T, Jacobs G, Ma W, Shafer WD, Gnanamani MK, Gao P, Kitiyanan B, Davis BH, Klettlinger JLS, Yen CH, Cronauer DC, Kropf AJ, Marshall CL (2013) Appl Catal, A 464-465:165.

[20] Iglesia E, Soled SL, Fiato RA, Via GH (1993) J Catal 143:345.

[21] Pawley GS (1981) J Appl Crystallogr 14:357.

[22] Bruker AXS, Karlsruhe, Germany. TOPAS V4: General profile and structure analysis software for powder diffraction data, (2008).

[23] Storsæter S, Borg Ø, Blekkan EA, Holmen A (2005) J Catal 231:405.

[24] Zou W Gonzalez RD (1992) J Catal 133:202.

[25] Cook KM, Perez HD, Bartholomew CH, Hecker WC (2014) Appl Catal, A   482:275.

[26] Kato T, Usami T, Tsukada T, Shibata Y, Kodama T (2016) J Nucl Mater 479:123.

[27] Borg Ø, Rønning M, Storsæter S, van Beek W, Holmen A (2007) Stud Surf Sci Catal 163:255.

[28] Jacobs G, Chaney JA, Patterson PM, Das TK, Davis BH (2004) Appl Catal,   A 264:203.

[29] Voronov A, Tsakoumis NE, Hammer N, van Beek W, Emerich H, Rønning M (2014) Catal Today 229:23.

[30] Jacobs G, Ji Y, Davis BH, Cronauer D, Kropf AJ, Marshall CL (2007) Appl Catal, A 333:177.

[31] Guczi L, Bazin D, Kov´acs I, Bork´o L, Schay Z, Lynch J, Parent P, Lafon C, Stefler G, Koppány Z, Sajó I (2002) Top Catal 20(1):129.

[32] Zsoldos Z, Hoffer T, Guczi L (1991) J Phys Chem 95:798.

[33] Guczi L, Hoffer T, Zsoldos Z, Zyade S, Maire G, Garin F (1991) J Phys Chem 95:802.

[34] Sun S, Fujimoto K, Yoneyama Y, Tsubaki N (2002) Fuel 81:1583.

[35] Qi Y, Ledesma C, Yang J, Duan X, Zhu YA, Holmen A, Chen D (2017) J Catal 349:110.

[36] Cheng J, Song T, Hu P, Lok CM, Ellis P, French S (2008) J Catal 255:20.

[37] van der Laan GP Beenackers AACM (1999) Cat Rev Sci Eng 41:255.

[38] Cheng J, Hu P, Ellis P, French S, Kelly G, Lok CM (2009) Surf Sci 603:2752.

[39] Li F, Jiang D, Zeng XC, Chen Z (2012) Nanoscale 4:1123.

[40] Ma X, Su H, Deng H, Li WX (2011) Catal Today 160:228.

[41] den Breejen JP, Frey AM, Yang J, Holmen A, van Schooneveld MM, de Groot FMF, Stephan O, Bitter JH, de Jong KP (2011) Top Catal 54:768.

[42] Iglesia E, Soled SL, Fiato RA (1992) J Catal 137:212.

[43]   Iglesia E (1997) Stud Surf Sci Catal 107:153.

[44]   Schanke D, Vada S, Blekkan E, Hilmen A, Hoff A, Holmen A (1995) J
       Catal 156:85.

Table 1: ICP-MS elemental analysis results

Catalyst	Concentration [% wt.]				Relative concentration		
	Al	Co	Mn	NM	Co:Al	Mn:Co	NM:Co
Co	29.5(15)	11.5(5)	-	-	0.39(3)	-	-
CoMn	27.6(11)	11.26(10)	2.77(6)	-	0.41(2)	0.246(6)	-
CoMnPt	27.2(8)	11.2(5)	2.81(13)	0.397(14)	0.41(2)	0.25(2)	0.036(2)
CoMnRe	26.2(13)	11.2(8)	2.8(2)	0.433(9)	0.41(4)	0.25(2)	0.039(3)
CoMnRu	26.8(7)	11.4(8)	2.9(2)	0.195(5)	0.42(3)	0.25(2)	0.0171(12)

Table 2: Catalyst characterisation results

| Catalyst | D [%] | | $d_{Co_3O_4}$[b] | a[b]* | TPR peaks [°C] | | | DoR |
	H_2[a]	XRD	[nm]	[Å]	$Co_3O_4 \rightarrow CoO$	$CoO \rightarrow Co^{(0)}$	Pre-reduced	[%]
Co	5.7	8.8	14.6(3)	8.0811(8)	320	491	569	79
CoMn	4.8	8.7	14.7(3)	8.0917(9)	323	496	569	70
CoMnPt	6.2	7.8	16.4(3)	8.0874(8)	269	406	517	92
CoMnRe	6.1	8.9	14.4(3)	8.0909(9)	325	423	511	92
CoMnRu	7.5	10.0	12.8(2)	8.0913(2)	252	445	497	97

[a] Measured by H_2-chemisorption. [b] Measured by XRD. *) Co_3O_4 unit cell parameter.
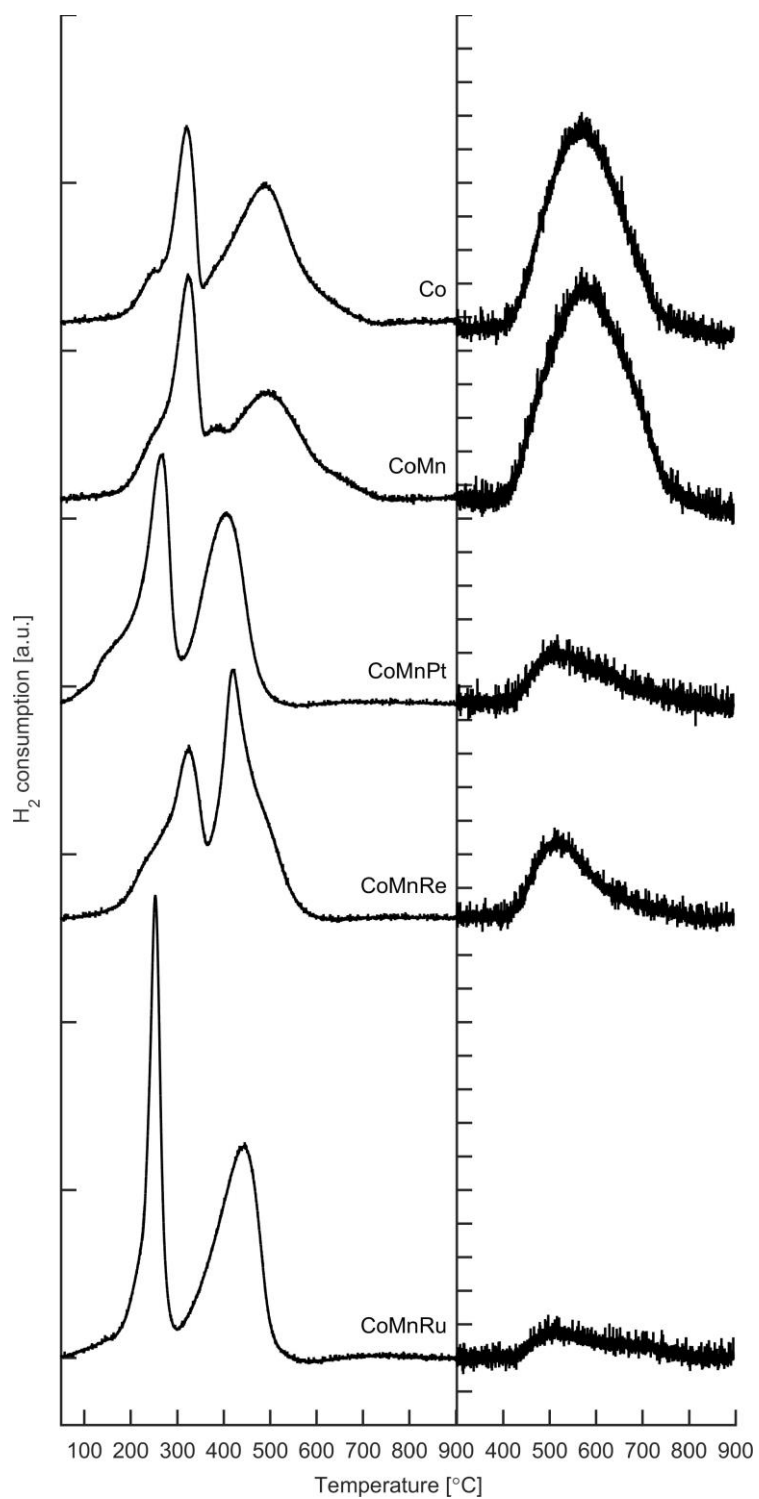
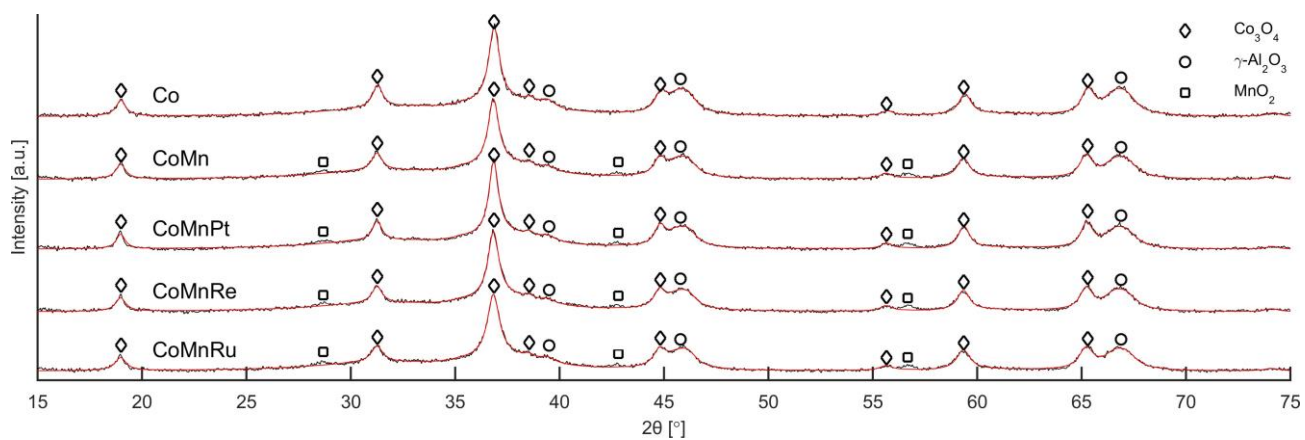Figure 1: Temperature programmed reduction profiles for calcined (left) and pre-reduced catalysts at 5×scale (right).

17

Figure 2: Background subtracted X-ray diffraction patterns (black) and full pattern fits (red) normalised to the γ-Al₂O₃ peak at 2θ = 66.9°.
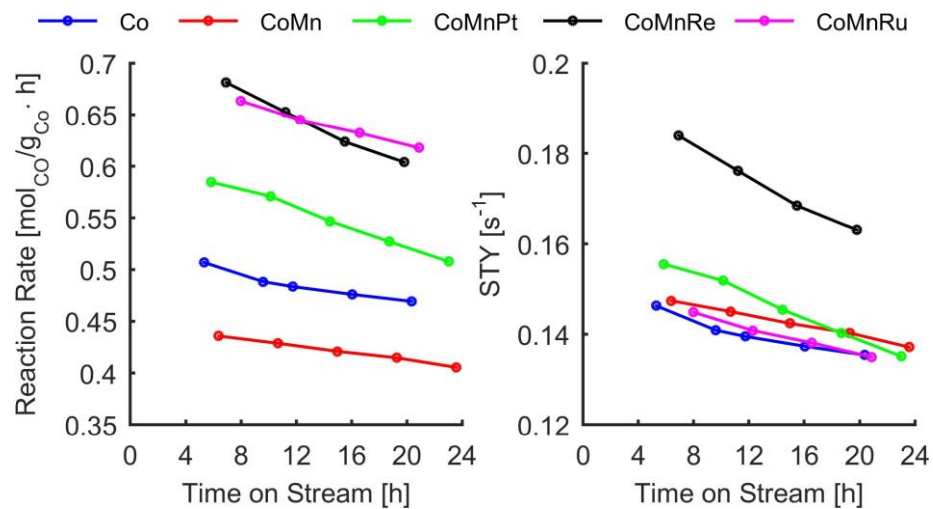
Figure 3: Co specific catalyst activity (left) and intrinsic activity (right).

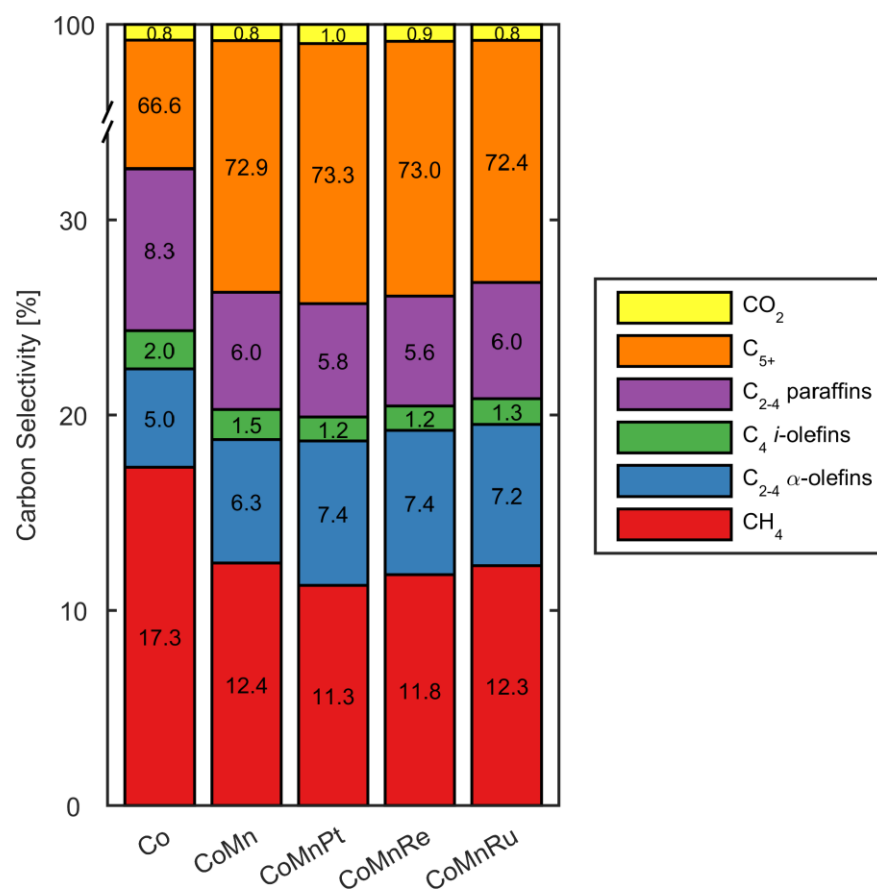Conditions: 240 $^\circ$C, 5 bara, H_2/CO = 2.1, GHSV = 15000 NmL/g_{cat}·h.

Figure 4: Catalyst carbon selectivity. Conditions: 240 $^\circ$C, 5 bara, H_2/CO = 2.1, CO conversion = 50 $\pm$ 2 %.
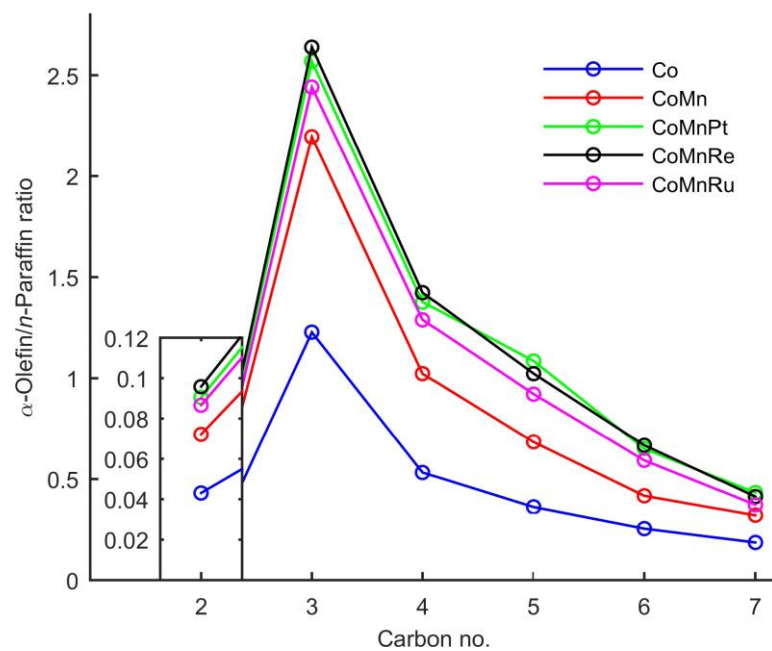
Figure 5: Gas phase α-olefin/*n*-paraffin ratios. C_2 emphasised at $10\times$scale. Conditions: 240 °C, 5 bara, $H_2/CO = 2.1$, CO conversion = 50 ± 2 %.